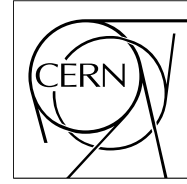


The Compact Muon Solenoid Experiment

**CMS Note**

Mailing address: CMS CERN, CH-1211 GENEVA 23, Switzerland



October 19, 2010

# Jet-veto Efficiency for the $WW$ production cross section in $pp$ collisions at $\sqrt{s} = 7$ TeV

D. Barge, C. Campagnari, P. Kalavase, D. Kovalskyi, V. Krutelyov, J. Ribnik

*University of California, Santa Barbara, Santa Barbara, USA*

W. Andrews, D. Evans, F. Golf, J. Mulmenstadt, S. Padhi, Y. Tu, F. Wurthwein, A. Yagil

*University of California, San Diego, San Diego, USA*

L. Bauerdick, I. Bloch, K. Burkett, I. Fis, Y. Gao, O. Gutsche, B. Hooberman

*Fermi National Accelerator Laboratory, Batavia, USA*

## Abstract

This note describes a data-driven method to estimate the jet-veto signal efficiency in data and its systematic uncertainties for the  $WW$  analysis. In this method, the  $WW$  jet-veto efficiency in data is parametrized as the product of the  $Z$  jet-veto efficiency in the data and the  $WW/Z$  jet-veto efficiency in the MC. We measure the  $Z$  jet-veto efficiency using the 3.1/pb data and compared to various MC samples. The dominant systematic uncertainty in the  $WW$  jet-veto efficiency is from the  $WW/Z$  jet-veto efficiency ratio estimation. The  $WW$  jet-veto efficiency is estimated as  $61.1 \pm 0.9 \pm 4.5$  % using the corrected PFJet at the jet-veto threshold of 25 GeV.

# Contents

<b>1</b>	<b>Introduction</b>	<b>2</b>
<b>2</b>	<b>Jet-veto Efficiency Measurement on <math>Z</math> data</b>	<b>2</b>
<b>3</b>	<b><math>WW/Z</math> Jet-veto Efficiency Ratio Estimate</b>	<b>7</b>
<b>4</b>	<b>Jet Response Validation Using <math>Z + 1</math> Jet Events</b>	<b>7</b>
<b>5</b>	<b>Summary and Conclusion</b>	<b>11</b>

## 1 Introduction

For the cross section measurement of  $pp \rightarrow WW \rightarrow 2l2\nu_l$  [1], one of the dominant backgrounds is the top-background. The only difference between the top-background and the  $WW$  signal is the presence of one or two extra  $b$ -jets in the final states. Thus, one efficient way to suppress the top-background is to apply jet-veto, vetoing the events with leading jet  $p_T$  above a threshold.

The uncertainties of jet-veto signal efficiency come from both the matrix element calculations and the jet reconstruction. In the leading order matrix element calculation, the  $pp \rightarrow WW \rightarrow 2l2\nu$  process does not contain jet. Extra jets are primarily due to the initial state radiation. It makes the jet energy spectrum sensitive to the corrections beyond the LO. On the jet reconstruction side, the effects from the jet energy correction and its uncertainties can propagate towards the jet-veto efficiency estimation as well. Validation of the jet response between the data and MC is thus required.

In this note, we describe a partially data-driven approach to measure the  $WW$  jet-veto signal efficiency. In this method, we exploit the similarity of the  $pp \rightarrow WW \rightarrow 2l2\nu_l$  and  $pp \rightarrow Z \rightarrow 2l$  processes. We estimate the jet-veto signal efficiency on  $WW$  as the jet-veto efficiency of  $pp \rightarrow Z \rightarrow 2l$  on data multiplied by the  $WW/Z$  jet-veto efficiency ratio estimated on the Monte Carlo, shown in Equation 1. Table 1 summarizes the data and MC samples used in this note.

$$\epsilon_{WW}^{data} \approx \epsilon_Z^{data} \times (\epsilon_{WW}^{MC}/\epsilon_Z^{MC}) = \epsilon_Z^{data} \times R_{WW/Z}^{MC} \quad (1)$$

## 2 Jet-veto Efficiency Measurement on $Z$ data

In this section, we describe the jet-veto efficiency measurement on the  $pp \rightarrow Z \rightarrow ll$ , comparing the data with various Monte Carlo samples (Table 1).

We use the same lepton selections as in the  $WW$  analysis to select the two leptons in the  $Z \rightarrow ll$  decays. Additional requirements to select the  $Z$  events are listed as follows,

- dilepton mass inside the  $Z$  mass window:  $|m_{ll} - m_Z| < 15\text{GeV}$ ;
- if more than one di-lepton candidates are selected in an event, the one with di-lepton mass closest to the  $Z$  mass is chosen

Aside from the maximum leading jet  $p_T$ , the choice of  $\eta$  range to which the jet-veto is applied is also important. Applying the jet-veto in the full  $\eta$  range ( $|\eta| < 5$ ) gives the best signal over background performance. Figure 1 shows the leading jet  $p_T$  in the region of  $3 < |\eta| < 5$ , and Figure 2 shows the respective jet-veto efficiencies and the MC/data ratios. We find the MC/data jet-veto efficiency ratios are close to unity for all the jet algorithms in all the MC samples considered. Therefore, we choose to apply the jet veto in the full  $\eta$  range  $|\eta| < 5.0$ .

Figure 3 shows the jet-veto efficiencies and the MC/data ratios, using the uncorrected JPT jets and PFJet [2]. We find similar performance between these two types of jets even without the jet energy correction. Figure 4 shows

Table 1: List of datasets

Luminosity	Collision Data
	Dataset
3.1	/EG_Run2010A-PromptReco-v4_RECO/
	/EG_Run2010A-PromptReco-v4_RECO/
	/EG_Run2010A-Jul16thReReco-v2_RECO/
	/EG_Run2010A-Jun14thReReco_v1_RECO/
	/MinimumBias_Commissioning10-SD_EG-Jun14thSkim_v1_RECO/
Monte Carlo	
Pythia	/Zee_Spring10-START3X_V26_S09-v1/
	/Zmumu_Spring10-START3X_V26_S09-v1/
	/WW_Spring10-START3X_V26_S09-v1/
Madgraph	/ZJets-madgraph_Spring10-START3X_V26_S09-v1/
	/VVJets-madgraph_Spring10-START3X_V26_S09-v1/
MC@NLO	/Zgamma_ee_M20-mcatnlo_Spring10-START3X_V26_S09-v1/
	/Zgamma_mumu_M20-mcatnlo_Spring10-START3X_V26_S09-v1/
	/WWtoEE-mcatnlo_Spring10-START3X_V26_S09-v1/
	/WWtoEPlusMuMinus-mcatnlo_Spring10-START3X_V26_S09-v1/
	/WWtoEPlusTauMinus-mcatnlo_Spring10-START3X_V26_S09-v1/
	/WWtoMuMu-mcatnlo_Spring10-START3X_V26_S09-v1/
	/WWtoMuPlusEMinus-mcatnlo_Spring10-START3X_V26_S09-v1/
	/WWtoMuPlusTauMinus-mcatnlo_Spring10-START3X_V26_S09-v1/
	/WWtoTauTau-mcatnlo_Spring10-START3X_V26_S09-v1/
	/WWtoTauPlusEMinus-mcatnlo_Spring10-START3X_V26_S09-v1/
	/WWtoTauPlusMuMinus-mcatnlo_Spring10-START3X_V26_S09-v1/

the jet-veto efficiencies using the L2L3 corrected CaloJet, TrkJet, PFJet and JPT Jets. The MC@NLO sample is found to have softer jet energy spectrum compared to data, yielding a larger jet-veto efficiency. The jet-veto efficiencies in the Pythia/Madgraph MC samples agree well with the data, with a discrepancy level of within 5%. The  $Z$  jet-veto efficiencies using the uncorrected and corrected PFJets at three different energy cut (20, 25, 30) GeV are tabulated in Table 2-3.

Table 2: Jet-veto signal efficiency on  $Z$  data and the MC/data ratios using the uncorrected PFJet.

Jet-veto Cut (GeV)	Pythia/Data (%)	Madgraph/Data (%)	MC@NLO/Data (%)	$\epsilon_Z^{data}(\%)$
20	100.4 $\pm$ 1.3	103.4 $\pm$ 1.4	107.3 $\pm$ 1.4	76.3 $\pm$ 1.0
25	100.7 $\pm$ 1.1	102.1 $\pm$ 1.1	105.1 $\pm$ 1.2	82.6 $\pm$ 0.9
30	100.2 $\pm$ 0.9	100.9 $\pm$ 0.9	103.5 $\pm$ 1.0	87.2 $\pm$ 0.8

Table 3: Jet-veto signal efficiency on  $Z$  data and the MC/data ratios using the corrected PFJet with L2L3, plus the residual corrections for data.

Jet-veto Cut (GeV)	Pythia/Data (%)	Madgraph/Data (%)	MC@NLO/Data (%)	$\epsilon_Z^{data}(\%)$
20	100.3 $\pm$ 1.5	104.8 $\pm$ 1.6	109.6 $\pm$ 1.7	71.3 $\pm$ 1.1
25	101.4 $\pm$ 1.3	103.7 $\pm$ 1.3	106.8 $\pm$ 1.3	78.8 $\pm$ 1.0
30	100.5 $\pm$ 1.0	101.8 $\pm$ 1.0	104.4 $\pm$ 1.1	84.5 $\pm$ 0.9

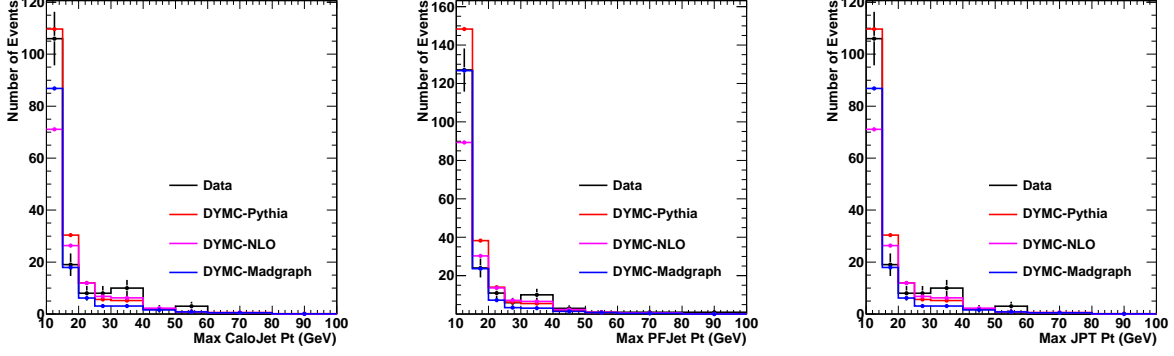


Figure 1: Left: The maximum energy of the calo jets with  $3 < |\eta| < 5$ . Middle: The maximum energy of the calo jets with  $3 < |\eta| < 5$ . Right: The maximum energy of the JPT jets with  $3 < |\eta| < 5$ . The MC samples are normalized to the data by the number of events in the full jet et range.

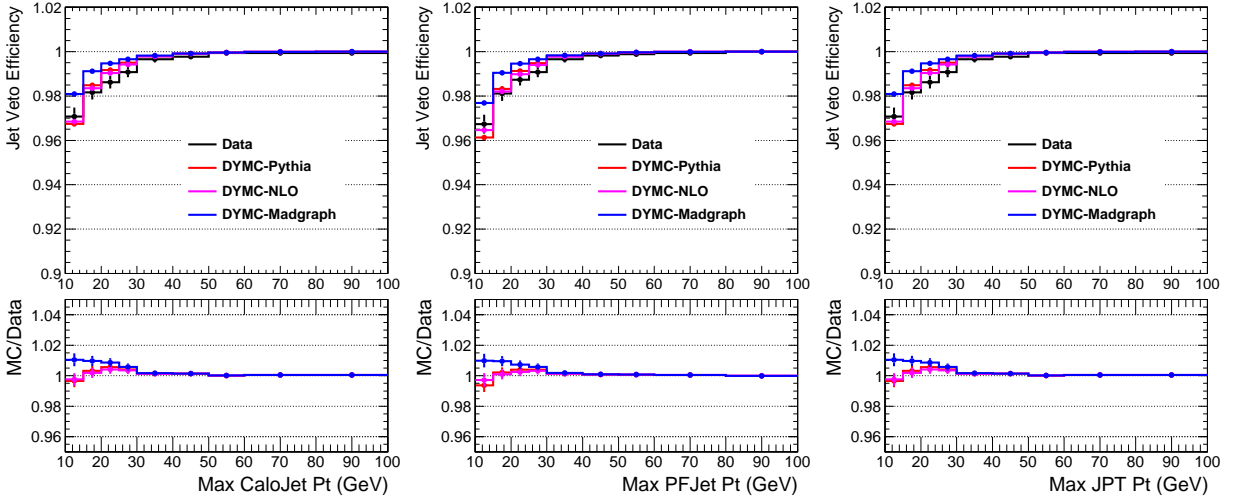


Figure 2: Left: The jet-veto efficiency of the calo jets with  $3 < |\eta| < 5$ . Middle: The jet-veto efficiency of the pf jets with  $3 < |\eta| < 5$ . Right: The jet-veto efficiency of the pf jets with  $3 < |\eta| < 5$ .

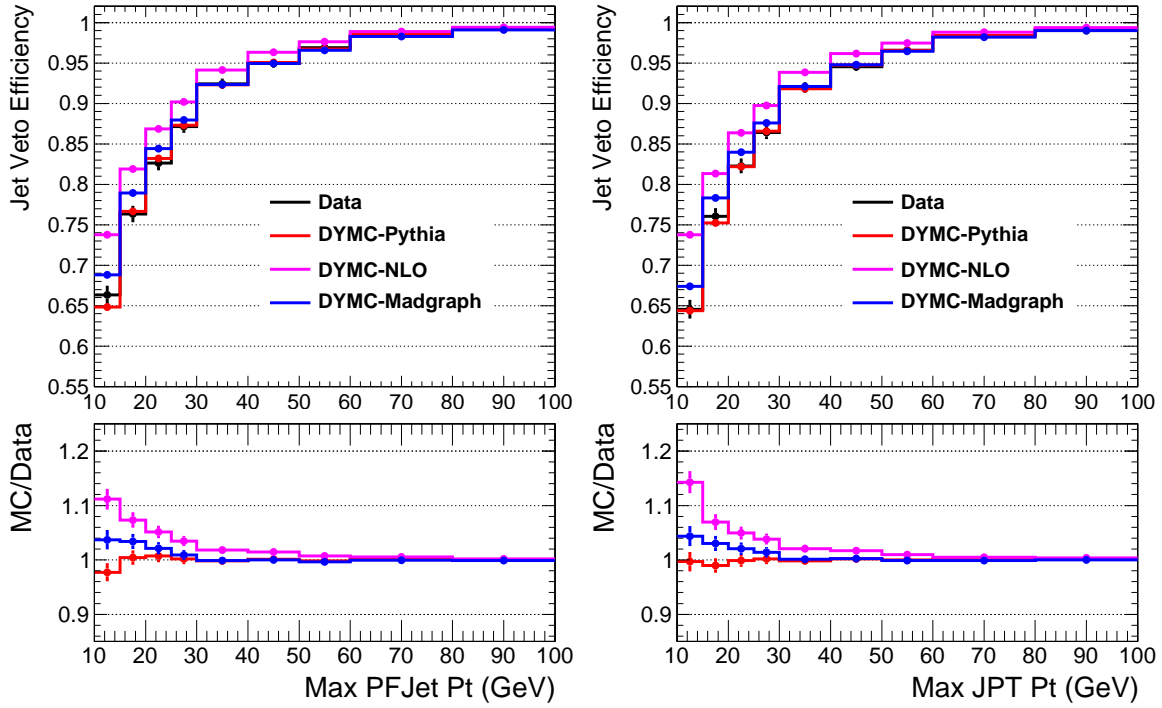


Figure 3: Left: The jet-veto efficiency of the pf jets with  $|\eta| < 5$ . Right: The jet-veto efficiency of the JPT jets with  $|\eta| < 5$ .

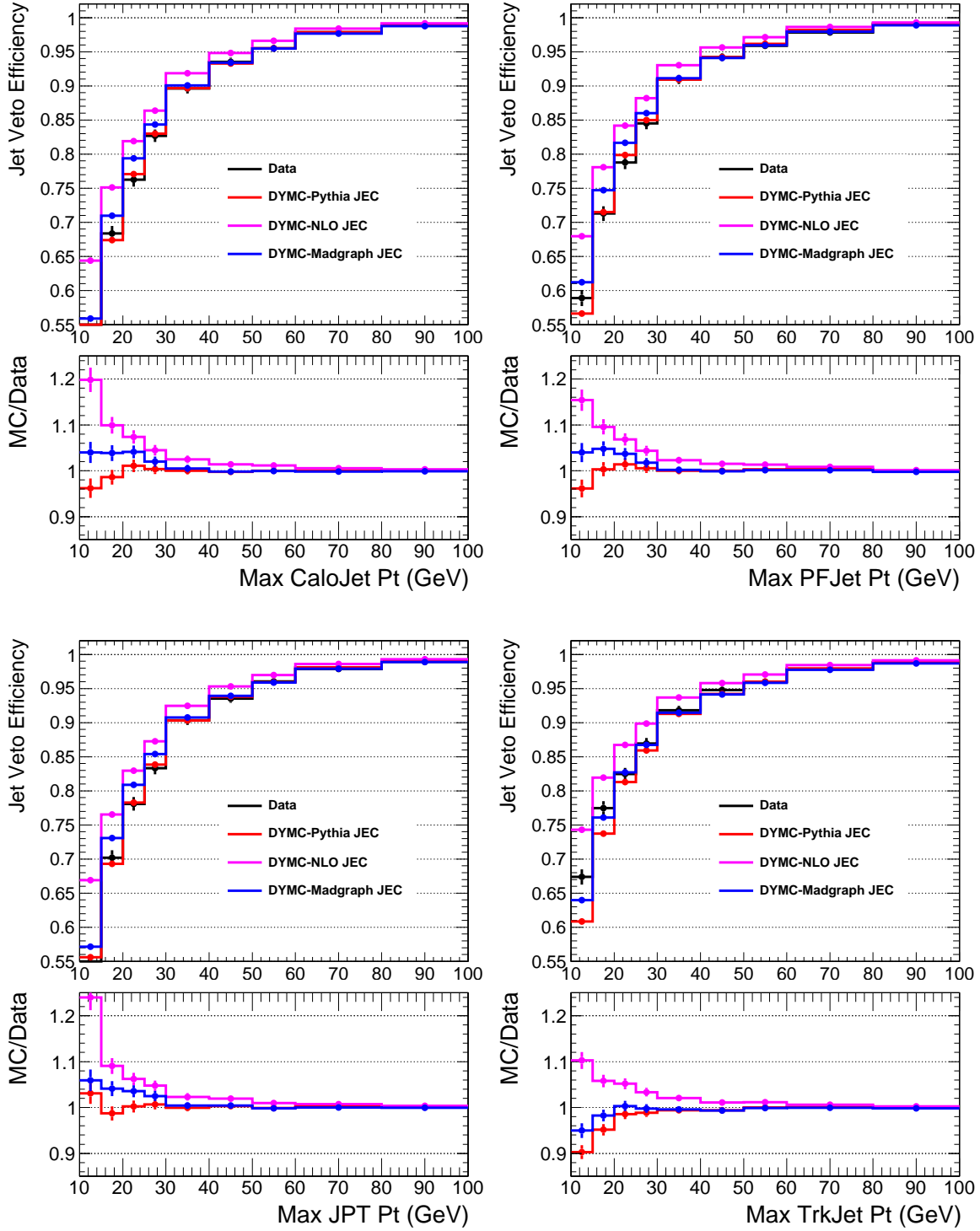


Figure 4: Left: The jet-veto efficiency of the pf jets with  $|\eta| < 5$ . Right: The jet-veto efficiency of the JPT jets with  $|\eta| < 5$ .

### 3 $WW/Z$ Jet-veto Efficiency Ratio Estimate

In this section, we describe the  $WW/Z$  jet-veto efficiency ratio  $R_{WW/Z}$  (Equation 1) estimation. The  $WW$  production has a different kinematic from the  $Z$ , as the energy scale in the former is much larger than the latter (see Figure 5, left). This indicates that the incoming partons  $q\bar{q}$  in the  $WW$  production have a larger energy on average than the  $Z$  productions. This results in a harder ISR parton energy spectrum, shown in Figure 5 (right).

Figure 6-7 show the  $WW/Z$  jet-veto efficiency ratio dependence on the leading jet  $p_T$ , using the uncorrected and corrected jets respectively. The predictions from the Madgraph agree with the MC@NLO within 1-2%. The predictions from the Pythia MC differ from the other two in the order of 10% on average. Note that the jet-veto efficiencies in the  $Z$  control region from Pythia and Madgraph MC samples agree within 3% (section 2). The large Pythia/Madgraph difference in the  $R_{WW/Z}$  is due to the different leading jet  $p_T$  spectrum in the  $WW$  productions. More specifically, Pythia predicts a much softer jet energy spectrum than Madgraph in the  $WW$  production.

In Pythia, the matrix element calculation for  $WW$  production includes only the leading order contributions. The ISR is modeled through the parton showering in the soft-collinear limit. On the other hand, both the Madgraph and mc@nlo MCs take into account upto 1 parton ISR in the matrix element calculation. The large Pythia/Madgraph difference could be due to the imperfect modelling of the ISR in Pythia parton showering. The good agreement between the Pythia and Madgraph in the  $Z$  jet-veto efficiency is likely because the Pythia parton showering is tuned well on  $Z$  region using data.

To disentangle the jet reconstruction differences, we studied the  $WW/Z$  jet-veto efficiency ratio dependence on both the generator level jet energy and the parton energy, shown in Figure 8. The large difference of the Pythia predictions from Madgraph and mc@nlo persists at the generator level. We use the MCFM[?] MC generator to probe the  $WW/Z$  jet-veto efficiency ratio dependence on the matrix element level parton energy. The events are generated with up to 1 extra parton in the final states. The parton  $p_T$  is taken as the magnitude of the recoiling four or two leptons  $p_T$  in the  $WW \rightarrow 2l2\nu$  or  $pp \rightarrow Z \rightarrow 2l$  decays.

Therefore, we choose the Madgraph as the MC sample to calculate the  $WW/Z$  jet-veto efficiency ratio  $R_{WW/Z}^{MC}$ . We assign half the Pythia/Madgraph difference as its systematic error. The  $R_{WW/Z}^{MC}$  results are tabulated Table 4-5 using the uncorrected and corrected PFJets for three different jet energy cut (20, 25, 30) GeV.

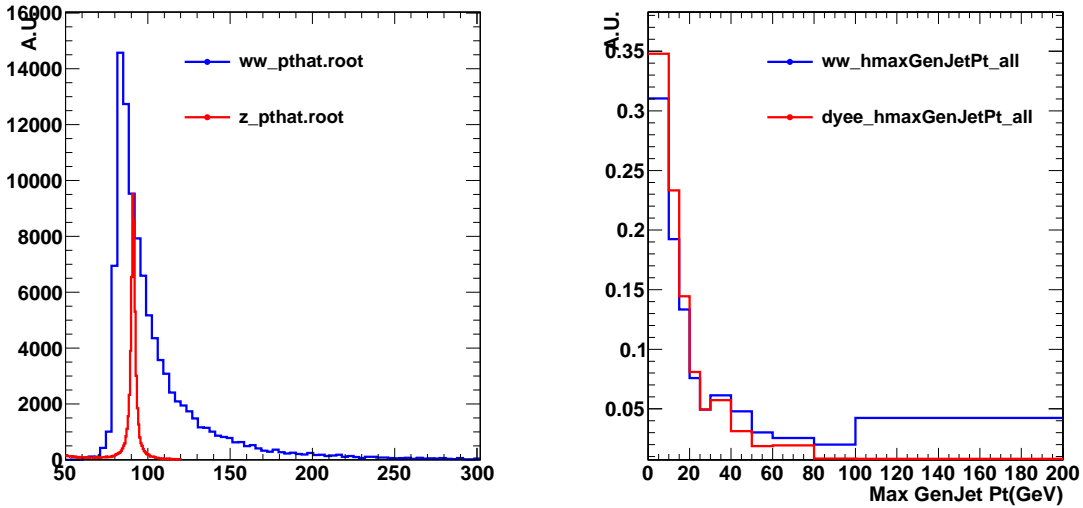


Figure 5: Left: The  $\hat{s}$  for the  $pp \rightarrow WW$  (Blue) and  $pp \rightarrow Z$  (Red). Right: The GenJet max jet energy spectrum for the  $pp \rightarrow WW$  (Blue) and  $pp \rightarrow Z$  (Red).

### 4 Jet Response Validation Using $Z + 1$ Jet Events

The jet energy correction [3] uncertainties give rise to additional uncertainties in evaluating both the  $Z$  jet-veto efficiency and the  $WW/Z$  jet-veto efficiency ratios.

The bulk of the jet energy correction are the L2L3 corrections, see Figure 9 (left). The same L2L3 corrections are

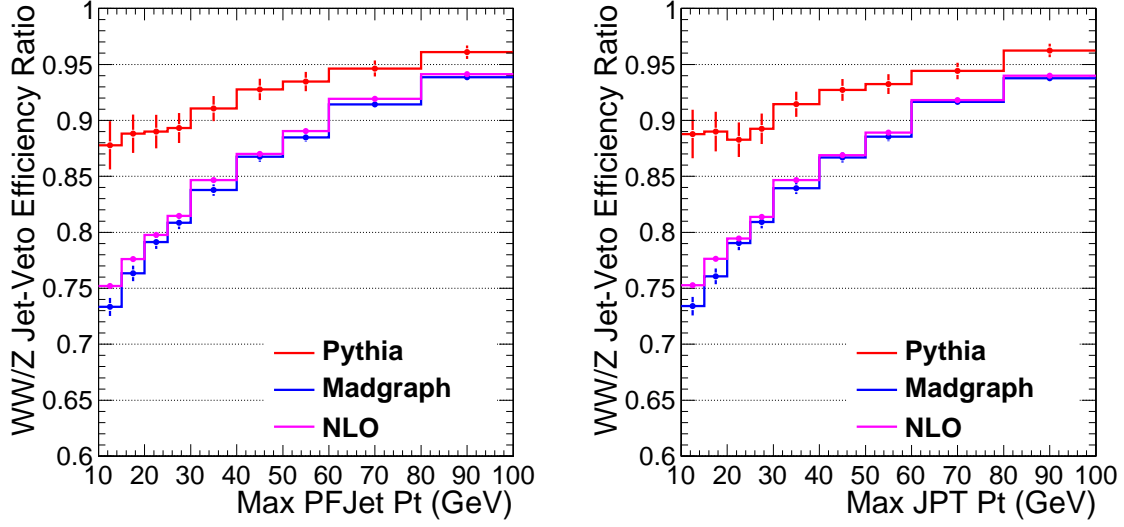


Figure 6: Left: The  $WW/Z$  jet-veto efficiency ratio  $R_{WW/Z}$  using the PFJet; Right: The  $WW/Z$  jet-veto efficiency ratio  $R_{WW/Z}$  using the JPT;  $R_{WW/Z}$  using the JPT;

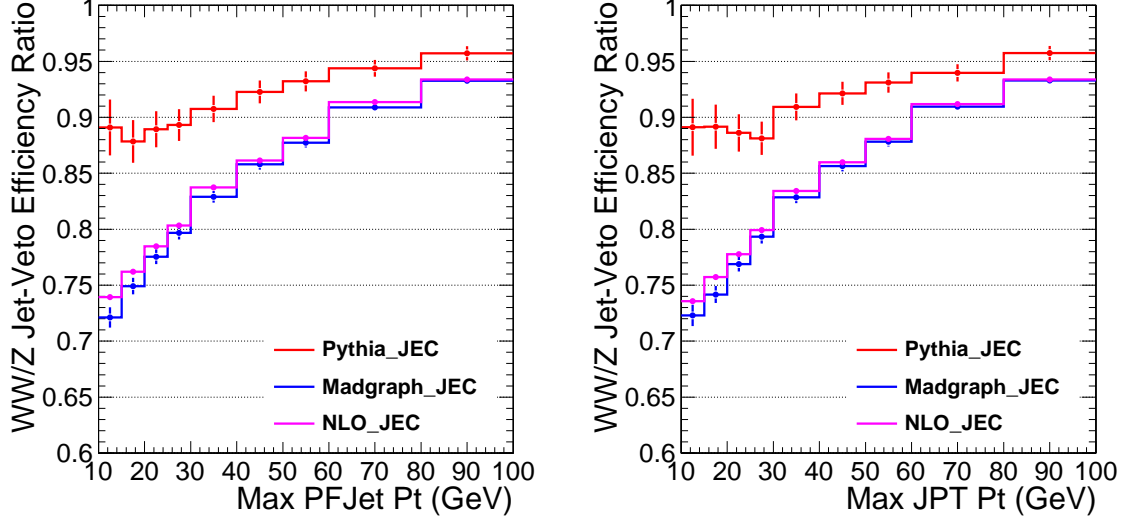


Figure 7: Left: The  $WW/Z$  jet-veto efficiency ratio  $R_{WW/Z}$  using the corrected PFJet; Right: The  $WW/Z$  jet-veto efficiency ratio  $R_{WW/Z}$  using the corrected JPT;

applied to both data and MC. For the data, additional residual corrections (Figure 9, right) are applied to improve the data/MC agreement [4]. The jet energy correction at the  $p_T$  range of (20-30) GeV are important for the jet-veto signal efficiency. As the jet energy corrections are primarily derived for the high  $p_T$  jets, we perform a simple cross check on the data/MC comparisons of the jet response, using the  $Z$ +jet events, similar to the method described in [5].

The  $Z$ +jet events are selected with the following two additional requirements beyond the selections described in section 2.

- The leading jet and the  $Z$  are back-to-back:  $|\Delta\phi(\vec{p}_{T,leadingjet} - \vec{p}_Z)| < 0.2$ ;
- The maximum  $p_T$  of other jets in the event is  $0.1 \times p_T(leadingjet)$ .

Figure 10 shows the jet energy scale derived from the  $Z$ +jet events for the PFJet. The jet energy scale is defined as the  $p_T(leadingjet)/p_T(Z)$ . We see a small systematic shift about 5% for the jets at  $p_T$  range of (20-30) GeV.



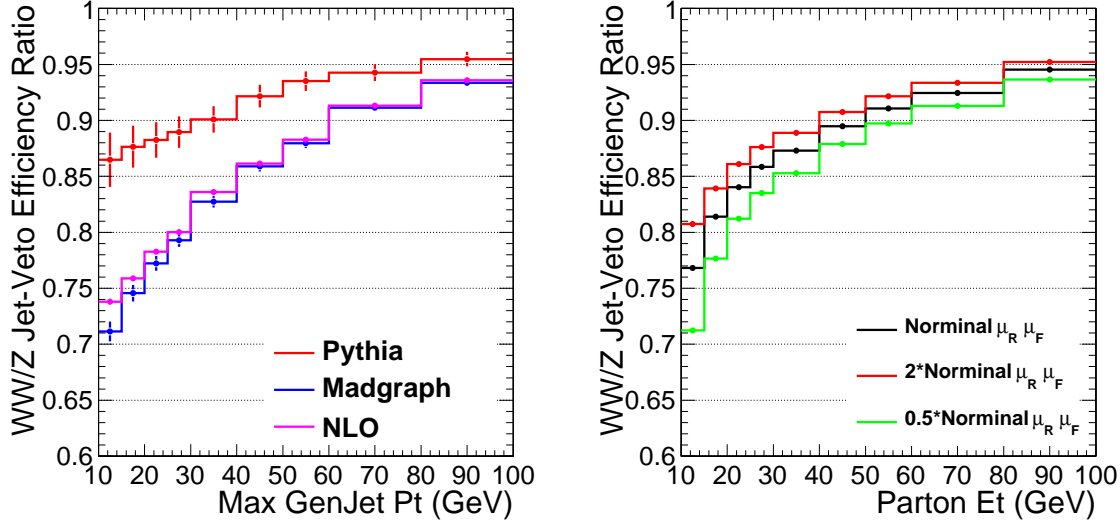


Figure 8: Left: The  $WW/Z$  jet-veto efficiency ratio  $R_{WW/Z}$  using the GenJet; Right: The  $WW/Z$  jet-veto efficiency ratio  $R_{WW/Z}$  using the parton  $p_T$ . The parton four-momentum is calculated as the sum of the four (two) leptons in the case of  $WW \rightarrow 2l2\nu_l$  ( $Z \rightarrow 2l$ ).

Table 4: The  $WW/Z$  jet-veto signal efficiency ratio using the uncorrected PFJet. The efficiency ratio is quoted as the value using PFCjets based on Madgraph MC sample. The uncertainty on  $R_{WW/Z}^M$  is taken as half of the difference between Pythia and Madgraph.

Jet-veto Cut (GeV)	$\sigma R_{WW/Z}^{MC}$ (%)
20	$76.3 \pm 0.7 \pm 6.2$
25	$79.1 \pm 0.6 \pm 4.9$
30	$80.9 \pm 0.6 \pm 4.2$

Table 5: The  $WW/Z$  jet-veto signal efficiency ratio using L2L3 corrected PFJet. The efficiency ratio is quoted as the value using PFCjets based on Madgraph MC sample. The uncertainty on  $R_{WW/Z}^M$  is taken as half of the difference between Pythia and Madgraph.

Jet-veto Cut (GeV)	$\sigma R_{WW/Z}^{MC}$ (%)
20	$74.9 \pm 0.7 \pm 6.5$
25	$77.5 \pm 0.7 \pm 5.7$
30	$79.7 \pm 0.6 \pm 4.8$

However, the data is statistically limited. Note that The efficiency difference for a correction around 11% (Figure 9, left) yields a difference about 4% in the  $Z$  jet-veto efficiency uncertainty and 1% in the  $R_{WW/Z}$ . We estimate that jet energy correction induced systematic uncertainty is less than 2%, assuming the jet energy correction uncertainty is 5%. For the time being, the contributions of this difference is ignored in the jet-veto efficiency estimation. We will repeat the study with more data and apply appropriate corrections based on more precise measurement of this data/MC shift.

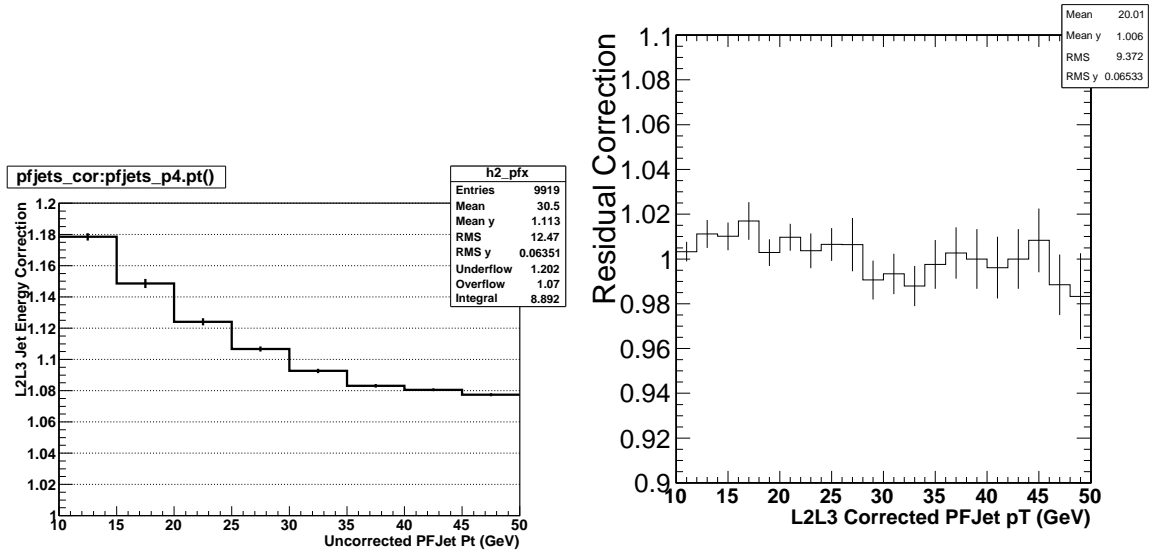


Figure 9: Left: The PFJet L2L3 jet energy correction. Right: The PFJet residual corrections derived for data.

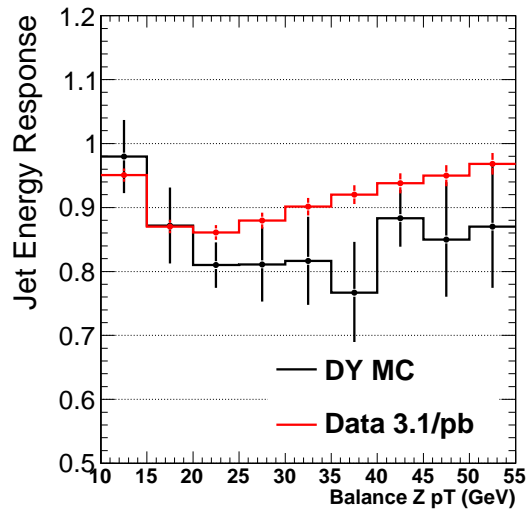


Figure 10: The jet energy scale derived from the  $Z$ +jet events for the PFJet.

## 5 Summary and Conclusion

In summary, we described a data-driven method to estimate the  $WW$  jet-veto signal efficiency and its systematic uncertainties. The  $WW$  jet-veto efficiency in data is parametrized as the product of the  $Z$  jet-veto efficiency in the data and the  $WW/Z$  jet-veto efficiency in the MC.

We have measured the  $Z$  jet-veto efficiencies in data and compared to various MC samples, shown in Table 2-3. We observed good agreement of  $Z$  jet-veto efficiency between data and the Pythia and Madgraph MC samples. We have studied the  $WW/Z$  jet-veto efficiency ratios using the Pythia, Madgraph and MC@NLO MC samples. The predictions from the Madgraph and MC@NLO MC samples are found to agree with each other within 1%. The jet energy spectrum in the Pythia MC is however significantly softer than the other two, yielding a difference of more than 10% at the jet  $p_T$  cut of 20 GeV. Based on the above findings, we choose the Madgraph as the nominal MC to calculate the  $WW/Z$  jet-veto efficiency ratio and assign half of the difference between the Pythia and Madgraph predictions as the  $R_{WW/Z}^{MC}$  uncertainties.

The  $WW$  jet-veto efficiencies using the uncorrected and corrected PFJet at  $p_T$  cut of (20, 25, 30) GeV are tabulated in Table 6-7.

Table 6: Jet-veto signal efficiency on  $WW$  using the uncorrected PFJet. Madgraph MC is chosen for the  $R_{WW/Z}^{MC}$

Jet-veto Cut (GeV)	$\epsilon_Z^{data}$ (%)	$R_{WW/Z}^{MC}$ (%)	$\epsilon_{WW}$ (%)
20	$76.3 \pm 1.0$	$76.3 \pm 0.7 \pm 6.2$	$58.3 \pm 0.9 \pm 4.8$
25	$82.6 \pm 0.9$	$79.1 \pm 0.6 \pm 4.9$	$65.4 \pm 0.9 \pm 4.1$
30	$87.2 \pm 0.8$	$80.9 \pm 0.6 \pm 4.2$	$70.5 \pm 0.8 \pm 3.7$

Table 7: Jet-veto signal efficiency on  $WW$  using the L2L3 corrected PFJet for both data and MC. For data, additional residual correction is applied as well. Madgraph MC is chosen for the  $R_{WW/Z}^{MC}$

Jet-veto Cut (GeV)	$\epsilon_Z^{data}$ (%)	$R_{WW/Z}^{MC}$ (%)	$\epsilon_{WW}$ (%)
20	$71.3 \pm 1.1$	$74.9 \pm 0.7 \pm 6.5$	$53.4 \pm 1.0 \pm 4.6$
25	$78.8 \pm 1.0$	$77.5 \pm 0.7 \pm 5.7$	$61.1 \pm 0.9 \pm 4.5$
30	$84.5 \pm 0.9$	$79.7 \pm 0.6 \pm 4.8$	$67.3 \pm 0.9 \pm 4.1$

## References

- [1] CMS AN -2009/042, “Prospects for measuring the  $WW$  production cross section in  $pp$  collisions at  $\sqrt{s} = 10$  TeV”
- [2] CMS PAS JME-07-003, “Performance of Jet Algorithms in CMS”
- [3] CMS PAS JME-10-003, “Jet Performance in  $pp$  Collisions at  $\sqrt{s} = 7$  TeV”
- [4] <https://hypernews.cern.ch/HyperNews/CMS/get/JetMET/1017.html>
- [5] CMS PAS JME-09-005, “Determination of the jet energy scale using  $Z \rightarrow e^+e^- + \text{jet}$   $p_T$  balance and a procedure for combining data driven corrections”, CMS PAS JME-09-009, “Calibration of the absolute jet energy scale with  $Z(\rightarrow \mu^+\mu^-) + \text{jet}$  events at CMS”